

AD-A140 875

LOW TEMPERATURE STRUCTURE AND PROPERTIES OF GRAPHITE  
LAMELLAR COMPOUNDS(U) NANCY-1 UNIV (FRANCE)  
D GUERARD ET AL. 1984 DAJ37-81-C-0045

UNCLASSIFIED

F / Q 20/2

NL



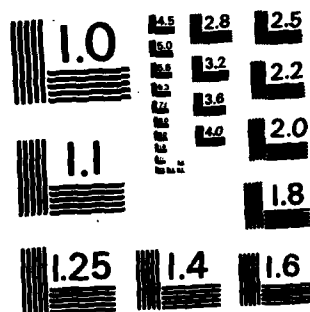
END

12471

9. 11. 2014

• • •

 $\cong \mathbb{P}^1$



MICROCOPY RESOLUTION TEST CHART  
NATIONAL BUREAU OF STANDARDS-1963-A

AD-A140 875

Universite de Nancy, France  
Title: Low Temperature Structure and  
Properties of Graphite Lamellar Compounds

EUROPEAN RESEARCH OFFICE

Contract DAJA 37-81-C-0045

FINAL REPORT

D. Guérard, A. Hérold, M. Lelaurain, E. McRae

1984

DTIC  
ELECTE  
S MAY 7 1984 D  
B

DISTRIBUTION STATEMENT A  
Approved for public release;  
Distribution Unlimited

The following researchers were also involved in the work of this contract :

Université de Nancy :  
(Laboratoire de Chimie  
Minérale Appliquée)

H. Fuzellier  
P. Lagrange  
J.F. Marêché  
N. Nadi  
C. Takoudjou  
R. Vangelisti

Université d'Orléans  
(Laboratoire de  
Cristallographie)

F. Rousseaux

Accession For	
NTIS GRA&I	<input checked="" type="checkbox"/>
DTIC TAB	<input type="checkbox"/>
Unannounced	<input type="checkbox"/>
Justification	
<b>PER FORM 50</b>	
By	
Distribution/	
Availability Codes	
Dist	Avail and/or Special
<b>A-1</b>	

## I. INTRODUCTION

The main initial objective of this E.R.O. supported research was a better understanding of the relationships between the structure and certain electronic properties of graphite intercalation compounds (GIC's) which might lead to the synthesis of compounds with a high electrical conductivity.

In order to achieve this, three kinds of research were developed

- 1) Much time was devoted to preparing samples of pure compounds, without macroscopic defects such as cleavages or curvatures, and with a mosaic spread as low as possible.
- 2) X-ray methods have been set up which permit a quantitative study of the defects in the compounds at room temperature and allow following the change in the structure from 300 K to about 10 K especially the variation of the identity period along the  $c$  axis perpendicular to the graphite sheets.
- 3) The in-plane electrical resistivity of several compounds was measured as a function of both stage and temperature, by using a contactless inductive method.

Throughout this work as far as possible, the results of these different studies have been compared not only with each other but also with those of other authors.

## II. EXPERIMENTAL TECHNIQUES

### II.1. Quantitative Recording of the Intensity Distribution Along an (hk) Rod perpendicular to the Layer Planes

Graphite intercalation compounds (GIC's) are never good single crystals. Two types of macroscopic defects hinder crystallographic analyses : the lack of layer planeness (e.g., puckering of the layers) and the presence of twinned domains. The method we have used allows for a quantitative correction of the effects of these defects.

This method was developed in collaboration with the Crystallography Laboratory at Orléans and is related to the precession method. Its advantage is that it allows access to the distribution of intensity along an (hk) rod using a classical diffractometer with an adjustable  $\Theta$ ,  $2\Theta$  movement. Details of the principle are given in Plançon et al. 1982.

### II.2. Low Temperature Setup for Transmission X-ray Diffraction

A drawing of the apparatus has already been presented in the first semi-annual report and is given again in figure 1.

The setup comprises a helium circulation cryostat with a large angular spread window. The measurements are carried out using a linear detector in conjunction with a multichannel analyzer linked to a screen, a rapid printer and an X-Y recorder.

Two goniometric units are used : one at the base which supports the cryostat and the arm of the detector (diffraction angle), the other at the top of the cryostat, rigidly linked with the sample (angle of incidence).

The X-rays (Mo-anticathode) are focused by a curved quartz monochromator. The radius of the focalization circle is 250 mm. In these conditions, the angular resolution is  $7/1000^\circ$  per channel.

The samples are protected by placing them in Lindemann glass tubes. The samples themselves are small plates ( $10 \times 1 \times 0.2 \text{ mm}^3$ ) or powders. They are surrounded by or mixed with diamond powder which is used as a reference, the advantage being that its cell parameter remains almost unchanged between 300 and 4 K. The tube is attached to a support at the extremity of the tail of the cryostat using "Cryophysics" varnish. A thermocouple is placed on the support just above the sample. A temperature controller allows regulating the temperature to within  $1/10^\circ$ .

### II.3. Electron Microscope

Electron diffraction offers an indispensable complement to the crystallographic study of certain GIC's. It allows observing the organization of the planar cells of the intercalant with respect to the cell of the graphite host. It also permits the observation of very small, single crystal, undeformed domains, of the order of a micron. Unfortunately, the introduction of very thin samples, alterable in air, remains a problem and renders an interpretation of the results somewhat difficult.

The microscope used was a JEOL 200CX (200 kV, 1.4 Å resolution), equipped with a goniometric head ( $\pm 60^\circ$ , 2 Å), a heater (1200°C) and a cooling plate (liquid nitrogen).

### II.4. Electrical Resistivity Measurements

For several years, the electrical transport measurements in our laboratory were limited to the temperature range 90 - 300 K (Mc Rae et al, 1980a). A helium circulation cryostat was then acquired which has allowed us to extend these measurements down to 4.2 K. The method has been adapted from our previous contactless technique, motivated by the considerable number of disadvantages of apparently simpler potentiometric methods which require contacts; reliable contacts are difficult to assure in practice because of the high anisotropy of these materials, the aggressivity of the intercalants and the considerable dilation of the sample upon reaction.

Aside from the cryostat itself, the setup comprises a well stabilized multi-frequency oscillator, a constant temperature regulator, an automatic control system for sample positioning, and the associated frequency and voltage measurement instrumentation. The technique is based on the principle that an air core solenoid loaded with a conductive, non-magnetic material undergoes a change in its initial complex impedance : the resistive portion increases due to eddy currents which flow in the sample and these eddy currents produce a magnetic field which opposes the initial flux of the solenoid thus decreasing the inductive portion of the complex impedance. If the solenoid forms part of the oscillator tank circuit, then the change in oscillator frequency  $\Delta\omega/\omega$  can be related to sample conductivity :  $\Delta\omega/\omega = f(\Delta R, \Delta j\omega L)$ .

The basic form of this relationship has been calculated from a theoretical view point and a considerable amount of calibration work has confirmed its validity. Direct current measurements were made with a number of metals in a four-point potentiometric configuration (Laplume, 1955), allowing us to determine with precision the variation  $\rho = f(T)$ . From the same metallic specimen, samples of the experimental geometry were cut (disks, 4 mm in diameter, 120-400 microns thick), and the frequency deviation  $\Delta f$  measured as a function of temperature and frequency. From these curves and the results of the four-point measurements, the relationship  $\Delta f = f(\sigma)$  could then



be determined. In the low conductivity region, the relationship is linear and in the high conductivity zone, the slopes  $d \Delta f / d\sigma$  become approximately equal, independent of sample thickness. These simplifications apply for the cases in which the skin depth,  $\delta$ , is either much greater than or smaller than the sample thickness,  $t$ , i.e.,  $\delta \gg t$  or  $\delta \ll t$ . In most instances we are interested in determining the bulk conductivity of our materials, so that it is the former which is of interest to us. The relationship then reduces to the form :

$$\rho = Kt / \Delta f,$$

where  $K$  is an experimentally determined parameter and also includes an  $S^2$  ( $S$  = sample surface area) term, which is constant in our case.

For the graphite acceptor compounds,  $\rho(4.2K) / \rho(300K) > 0.1$  for most compounds studied to date. This conductivity increase upon decreasing the temperature is accommodated for by having built the oscillator capable of functioning over a range of frequencies; by a proper choice of sample thickness, we can therefore always confine operation to the region for which  $\delta \gg t$ .

### III. RESULTS : DONOR COMPOUNDS

#### III.1. Room temperature disorder in heavy alkali metal compounds

The ideal stacking order for the first stage compound  $KC_8$  is :

$A\alpha A\beta A\gamma A\phi A\alpha$  where A represents the carbon planes and  $\alpha, \beta, \gamma$  and  $\phi$ , the relative in-plane positions of the alkali metal atoms (Lagrange et al 1978). There are, however, stacking defects e.g.  $A\alpha A\alpha A\beta A\gamma A\phi A\alpha...$  The probability of such defects is  $n \sim 0.1$  (Rousseaux et al 1981a).

For the second stage compounds, not all the metal atoms are in registry with respect to the carbon atoms. This is shown by the absence of (hko) or (hkl) reflexions other than those relative to the graphite matrix.

A room temperature scanning along the (10  $\bar{1}$ ) and (11  $\bar{1}$ ) rods of the graphite matrix shows the presence of another type of defect : the ratio  $x : \frac{C}{M}$  where M represents the metal atoms located in the potential wells of graphite may vary (Rousseaux et al 1983).

The following table shows the values of x and  $\eta$  which allow the fitting of the experimental intensities :

Compound	x	% metal atoms in registry	$\eta$
$KC_{24}$	36	66	.33
$RbC_{24}$	48	50	.50
$CsC_{24}$	72	33	.50

Table 1. Values of x and  $\eta$  which allow the fitting of the experimental data relative to the (10 1) and (11  $\bar{1}$ ) reflexions for the second stage compounds  $MC_{24}$  of the heavy alkali metals.

The values of x show that, depending on the metal, there are only 1/3 to 2/3 of the intercalated atoms registered on the carbon planes.

This result reconciliates the different previous models which were based on either "liquid" or "gas" like intercalated layers. The truth is probably a mixture

between these two and it seems that at 300 K, the 2D melting process has already started for the three compounds.

As concerns  $\eta$ , its value is much larger for the second stage compounds ( $\eta = 0.33$  for  $KC_{24}$ ) than for  $KC_8$  ( $\eta = 0.1$ ) (Rousseaux et al. 1983).

### III.2. c axis thermal expansion of the compounds

#### III.2.1. Introduction

The aim of this study was the determination of the charge transfer in the graphitides by comparison of the dilatations of the intercalated and free metal and of the ion.

This study comprises four parts :

- measurement of the dilatation of the different graphitides with the apparatus described in the first part of this report.
- calculation of the thermal expansion of the intercalated species.
- determination of the thermal expansion of the  $M^+$  ions (which is not available in the literature). This part is described in the appendix.
- comparison of the expansion of the intercalated species with that of free metal and ion.

#### III.2.2. Experimental results

The compounds studied belong to the 1st. stage

- $MC_6$  ( $M = Li, Ba, Eu, Yb$ )
- $MC_8$  ( $M = K, Rb, Cs$ )

Two other compounds of potassium were also measured :  $KC_{24}$  (2 nd Stage) and  $KC_{48}$  (4 th stage). For these last two, the synthesis was carefully done in order to have :

- . a very well defined stage, especially without any "interstratification"
- . a minimum mosaic spread ( $< 1^\circ$  for  $KC_{48}$ )

The experimental variations of  $\frac{\Delta L_c}{L_c}$  versus temperature (figures 2, 3 and 4) present, either for the graphite itself or for the compounds, the same shape, with between about 100 and 300 K, a quasi-linear portion which allows us to calculate the expansion coefficient  $\bar{\alpha}$ .

The curve relative to the second stage compound  $KC_{24}$  (fig. 4) presents a step around 130 K. It corresponds to one of the resistivity anomalies shown by (Ogg et al. 1977).

The values of  $\bar{\alpha}$  are indicated in table 2.

### III.2.3. Discussion

In some cases ( $\text{LiC}_6$ ,  $\text{KC}_8$ ,  $\text{RbC}_8$  and  $\text{KC}_{24}$ ), the values of  $\bar{\alpha}$  are between that of the free metal and that of graphite; for the others, this value is smaller than both of these. It seems then, a priori, difficult to interpret this expansion in terms of partial ionization of the metal, unless that of the ion is very small, which is not the case, as shown in the appendix.

### III.2.4. Calculation of the dilatation of the intercalated species

These results will be presented at "Carbone 84" (Bordeaux, France 2.6 July 1984).

In order to determine that part of the expansion which is due to the metal itself, one has to take into account the relative sizes of graphite and intercalant units. In order to do so, we considered the model shown in fig. 5. The dilatation of the metal,  $\alpha_M$ , as a function of that of graphite  $\alpha_c$  and  $\bar{\alpha}$  is given by the relation :

$$\alpha_M = \frac{di}{r} \times \frac{\sqrt{4r^2 + 4rx - 3x^2}}{4r + 2x} \left[ \bar{\alpha} - \frac{2y}{di} \alpha_c - \frac{2r - 3x}{\sqrt{4r^2 + 4rx - 3x^2}} \frac{x}{di} \alpha_a \right] \quad (1)$$

where  $di$  is the interplanar distance,  $r$  the radius of the intercalated metal,  $\alpha_a$  is the in-plane expansion of graphite. This value is very small compared to  $\bar{\alpha}$  and to the expansion  $\alpha_c$  along the  $\vec{c}$  axis of graphite and was therefore neglected.

The relation used for the calculations of  $\alpha_M$  is :

$$\alpha_M = \frac{di}{r} \times \frac{\sqrt{4r^2 + 4rx - 3x^2}}{4r + 2x} \left[ \bar{\alpha} - \frac{2y}{di} \alpha_c \right] \quad (2)$$

### III.2.5. Charge transfer calculation

This was done only in the case of the first stage graphitides of the alkali metals.

Compound	$\times 10^{-6} \text{ K}^{-1}$					% ionic
	$\bar{\alpha}$ compound		$\alpha_M$ intercalated	$\alpha_M^\circ$	$\alpha_M^+$	
LiC <sub>6</sub>	31 $\pm$ 2	65(*)	18	51	11.9	82.9
BaC <sub>6</sub>	10 $\pm$ 2		3.1	25		
EuC <sub>6</sub>	12 $\pm$ 2		1.9	31		
YbC <sub>6</sub>	20 $\pm$ 2		12			
KC <sub>8</sub>	39 $\pm$ 2	45(**)	39.3	84	27.5	79.1
RbC <sub>8</sub>	33 $\pm$ 2	30(**)	36.4	86	33	93.5
CsC <sub>8</sub>	19 $\pm$ 2	28(**)	18.3	90	36	>100

(\*) Rossat-Mignod et al 1982

(\*\*) Hardcastle and Zabel 1983.

**Table 2.** Expansion coefficients of the compounds, intercalated, free metal, ion and charge transfer in the graphitides.

In order to determine the ionic character of the intercalated metal, we supposed the thermal expansion to be a linear function of the charge. These values are thus approximate, however, the calculated expansion of Cs in CsC<sub>8</sub> is much smaller than that of graphite, the free metal and the ion. It is thus impossible to explain the expansion in terms of an ionic bond between graphite and cesium.

### III.2.6. Stages 2 and 4 of potassium

Fig. 4 shows the variation of  $\frac{\Delta I_c}{I_{c295}}$  versus temperature for KC<sub>8</sub> (stage 1), KC<sub>24</sub> (stage 2) and KC<sub>48</sub> (stage 4). From the quasi-linear part of the curves, we determined  $\bar{\alpha}$ .

If one considers  $\bar{\alpha}$  to be the sum of contributions from the intercalated sandwich and graphite, one can calculate the expansion relative to these compounds :

Compound	$\alpha \cdot 10^{-6} \text{ K}^{-1}$	
	$\bar{\alpha}_{\text{exp.}}$	$\alpha_{\text{calc.}}$
KC <sub>8</sub>	38.4	
KC <sub>24</sub>	31 $\pm$ 2	33.6
KC <sub>48</sub>	26 $\pm$ 2	30.6

**Table 3.** Expansion of stage 1, 2 and 4 compounds of potassium.

The agreement is good for the stage 2 compound; it is slightly poorer although compatible with the experimental error for the higher stage compound.

This agreement would prove that the bonding within the sandwich is of the same type for all compounds. However, it is known that the charge transfer, smaller than one in the first stage compounds approaches unity in the higher stages.

### III.3. Conclusion

This study has provided experimental values of the thermal expansion of the graphitides along the  $\vec{c}$  axis.

We had hoped to be able to determine the charge transfer from these values. The very low expansion coefficient of some of the graphitides shows that the bond cannot be interpreted only in terms of an ionic bond. The case of cesium is particularly puzzling, since this is the most electropositive metal yet it gives the poorest agreement to an ionic model.

### III.4. Diverse

The work presented here has been made possible with the help of the contract; it will be completed through the study of other compounds.

For this purpose, we need to increase the variety of samples examined. We has already looked at some of them, in particular the hydrurographitides, but the preparation of such samples by the classical method is very long and we tried to set up a new method for the synthesis. This was done by C.Takoudjou who was paid in part by the contract.

He set up a new method which led, in a short time to the expected compound (2 nd stage) and also discovered the means of preparing the 1 st stage compound (Takoudjou 1983, Guérard et al. 1983).

#### IV. RESULTS : ACCEPTOR COMPOUNDS

##### IV.1. Compound Syntheses

All compounds were prepared by directly reacting the halide vapour with pyrographite (HOPG) in the presence of an excess of chlorine, but without the intervention of any other elements. It should, however, be noted that the preparation conditions can influence the chemical composition of the final product.

##### IV.2. Radiocrystallographic Studies

###### IV.2.1 FeCl<sub>3</sub>

The iron trichloride compounds were studied in depth at ambient temperature (Rousseaux et al. 1981b, 1982) inasmuch as the numerous previous works did not allow drawing any firm conclusions as to the arrangement of the graphite layers in the compound or to the nature of the defects which are always present to a significant degree in this type of compound.

Through a quantitative study of the correlations between layers in first and second stage compounds (Rousseaux et al. 1982), we have shown that the anomalies observed on X-ray diffraction diagrams can be explained by the existence of imperfect structural organization.

The layers of FeCl<sub>3</sub>, of hexagonal structure, intercalate with an orientation of 30° of their planar cell with respect to that of graphite :  $a_{\text{FeCl}_3} = 6.12 \text{ \AA} \pm 0.01$  instead of 6.06 Å for the free chloride;  $a_{\text{graphite}} = 2.454 \text{ \AA} \pm 0.001$  instead of 2.416 Å.

In the first stage compound of formula  $\text{C}_{6.6}\text{FeCl}_3$ ,  $I_c = 9.385 \pm 0.005 \text{ \AA}$  and in the second stage product  $\text{C}_{13.2}\text{FeCl}_3$ ,  $I_c = 12.73 \pm 0.02 \text{ \AA}$ .

Quantitative analysis reveals that even in pure phase GIC's, order almost never exists in the successions of intercalant layers. The best description is provided by a model consisting of random translation faults with a probability greater than 0.5. Thus the correlations between the carbon layers are modified. Analysis of the second stage GIC shows that the matrix is heterogeneous, although the predominant arrangement remains the AB type. This type of structural organization results from the forced adaptation of two incommensurable macromolecular lattices which is also the origin of the large mosaic spread observed particularly in FeCl<sub>3</sub> GIC's.

The significant mosaic spread and the difficulty of synthesizing pure stage compounds with high quality pyrographite explain why these materials were not retained for the initial low temperature studies.

In 1982, Mazurek et al. published the results of a low temperature crystallographic study on an impure first stage  $\text{FeCl}_3$  GIC. We have indicated their experimental values (dashed curve) in fig. 6. The coefficient of expansion which can be calculated based on this curve and on the interatomic distances indicated by the authors is  $35.5 \cdot 10^{-6} \text{ K}^{-1}$  and not  $25.5 \cdot 10^{-6} \text{ K}^{-1}$ . We believe that extrapolation of the results to higher stage compounds is incorrect inasmuch as it does not take into account the contraction of the parameter  $\vec{c}$  which is always observed for  $n \geq 2$  ( $n$  = stage) in metal halide GIC's.

At the temperature of liquid nitrogen, the electron microscope diffraction patterns do not show any changes with respect to the organization of the plane intercalant cell.

#### IV.2.2 $\text{AlCl}_3$

The structure of the first stage compound, approximately  $\text{C}_9\text{AlCl}_3$ , has not been completely defined. The intercalant is either organized or not between the carbon layers; fine measurements of the positions of the 001 reflexions have shown different values of the interplanar distance in the two cases,

When the intercalant is ordered,  $I_c$  can attain the value  $9.59 \pm 0.01 \text{ \AA}$ ; if not, then  $I_c = 9.52 \pm 0.01 \text{ \AA}$ . In most compounds, coexistence of the two phases is observed. The preparation conditions which lead to the formation of one or the other of these phases are currently under study. It has proved possible to study the contraction of the interplanar distance since intercalation does not deform the graphite layers and the mosaic spread is very low. On fig. 6, two curves of  $\Delta L/L_{295}$  have been given as a function of temperature. It is noted that the coefficient of thermal expansion is higher when the compound is organized:  $\alpha$  attains  $45 \cdot 10^{-6} \text{ K}^{-1}$ . A low temperature study of the compounds for  $n > 1$  will be undertaken in the future. At room temperature (fig. 7), it is noted that the interplanar distance varies enormously with stage.

#### IV.2.3. $\text{GaCl}_3$

The first stage compounds of limiting composition  $\text{C}_{9.8}\text{GaCl}_{3.45}$  (Nadi 1983 : Nadi et al. 1983) are constituted, at room temperature, of an A/A/A stacking of the carbon layers between which the trihalide seems to be randomly arranged, as manifested by recordings of the  $hk0$  and  $hkl$  reflexions carried out on a  $\text{GaCl}_3$  pyrographite compound (fig. 8a). The interplanar distance is equal to  $9.54 \pm 0.01 \text{ \AA}$ .



When this compound is cooled, bidimensional organization of the intercalant is observed below 230 K. Three dimensional order appears below 160 K (fig. 8b). A large number of hkl reflexions were recorded. While it can be affirmed that the parameter  $\vec{c}$  is equal in this case to  $2 \times I_c$ , uncertainty remains as to the dimensions of the plane cell. The X-ray diffraction pattern of a saturated, first stage product shows a greater number of reflexions than do the electron microscope patterns of poorer products. While, in this latter case, a parameter  $a = a/7$  times that of graphite is observed, the existence of a larger cell cannot be excluded for the richest compounds; this can only be defined by carrying out a low temperature structural study on single crystals.

For the first stage compound, we have measured the variation of the interplanar distance as a function of temperature (fig. 6). On the linear portion of the curve, the coefficient of expansion is  $\alpha = 29 \cdot 10^{-6} \text{ K}^{-1}$ , close to that of graphite.

As regards the higher stage compounds, other than the differences which have just been indicated concerning the organization of the intercalant at low temperatures for saturated and unsaturated compounds, the large variation in interplanar distance should be noted (fig. 7), as for the  $\text{AlCl}_3$  GIC's.

#### IV.2.4. Dichlorides

At room temperature, the structural analyses carried out by X-ray and electron diffraction have shown that these compounds are three dimensionally ordered but nevertheless contain defects. A complete crystallographic study is currently in progress.

We have followed the low temperature changes of the interplanar distance of the first stage compounds based on pyrographite with  $\text{CoCl}_2$  and  $\text{CdCl}_2$ . These results are presented on fig. 9. This figure suggests the existence of transitions for the  $\text{CoCl}_2$  GIC.

#### IV.3. Studies of the Basal Plane Electrical Resistivity

The most comprehensive study was made on  $\text{GaCl}_3$  intercalated graphite. In fact, this work comprises a wider range of stages than any other examination of GIC's. A more limited range of iron, aluminium and thallium trichloride compounds are also included.

Detailed results can be found elsewhere (McRae 1982, Maréché et al. 1983, Nadi 1983). The principal conclusions can be summarized as follows, with reference to Table 4 and figures 10 and 11.

1. As regards room temperature values of  $\text{GaCl}_3$  GIC's, the curves of  $\rho_{\text{GIC}}$  versus stage index (fig. 10a) show a broad minimum at  $n \sim 4$  where  $\rho_{\text{GIC}} \sim 3.2 \mu\Omega \text{ cm}$ , twice the resistivity of copper and only slightly greater than that of aluminum.

2. For both  $\text{GaCl}_3$  and  $\text{AlCl}_3$  GIC's, the conductivity gain through intercalation,  $(\sigma_{\text{GIC}}/\sigma_{\text{graph}})$  (fig. 10b) increases from  $n = 1$  to 4 or 5 then decreases. Our measurements on  $\text{FeCl}_3$  products show a decrease in this parameter as  $n$  increases. As noted in § IV.2.1-3, while  $\text{GaCl}_3$  allows intercalation to pure, high stage materials, it is very difficult to isolate pure  $\text{FeCl}_3$  GIC's for  $n \geq 3$ .

3. The lower curve of fig. 10a shows that the residual resistivity,  $\rho_{\text{res}}$  always lies between 0.5 and  $1 \mu\Omega \text{ cm}$ , remains fairly constant with increasing intercalant concentration for  $n \geq 4$  then gradually rises as the compound becomes increasingly saturated in the trichloride.

4. Table 4 illustrates the general increase in residual resistivity ratio  $(\rho_{300\text{K}}/\rho_{4.2\text{K}})_{\text{GIC}}$  as  $n$  rises. The values noted here are comparable to what is noted elsewhere for  $\text{SbF}_5$  - ( $n = 1 - 4$ ) and  $\text{HNO}_3$  GIC's ( $n = 1, 2$ ) (Wu et al. 1981) and  $\text{AsF}_5$  GIC ( $n = 1 - 4$ ) (Zeller et al. 1979). The particularly high values for some of the  $\text{GaCl}_3$  - poor compounds are to be noted.

5. Table 4 further shows that the  $\text{TlCl}_3$  material possesses an exceptionally high value of both room temperature and residual resistivity.

6. Fig. 11 illustrates that amongst the materials studied, none exhibit truly linear  $\rho$  versus  $T$  behaviour as would be expected for simple metals obeying the Bloch Gruneisen relationship. Here again, this is typical of the whole class of GIC's. The transitions noted for the 7th stage compound are quite remarkable since they were not noted in either poorer or richer materials.

Intercalant	n	$\rho_0$	GIC		
			$\rho_{300}$	$\rho_{res.}$	RRR
GaCl <sub>3</sub>	1	41.8	4.6	0.95	4.8
	3	39.0	3.7	0.85	4.4
	4	36.8	3.2	0.80	5.0
	5	46.0	4.0	0.65	6.1
	6	37.1	4.0	0.72	5.6
	7	36.9	5.7	0.92	6.2
	9	41.2	6.6	.65	10.2
	10	38.9	5.5	0.75	7.3
	11	37.9	9.5	0.77	12.3
	13+graph	38.4	8.5	0.98	8.7
FeCl <sub>3</sub>	2	46.9	5.3	0.76	7.0
	4	39.6	5.4	1.05	5.1
	6	44.6	5.9	-	-
AlCl <sub>3</sub>	1	38.9	4.1	-	-
	2	40.5	4.0	-	-
	4	37.8	3.5	-	-
TlCl <sub>3</sub>	2	43.7	12.0	2.0	6.0

**Table 4.** Data relative to  $\rho$  (T) studies on metal trichloride compounds. All values of  $\rho$  in  $\mu\Omega$  cm.  $\rho_0$  = resistivity of initial graphite sample.

#### IV.4. Discussion of Acceptor Compounds

The particularly high values of both room temperature and residual resistivity of the  $\text{TlCl}_3$  compound can be correlated with the exceptionally large increase in mosaic spread provoked by the intercalation process which appears to be much more destructive than in the case of the other group III B trichlorides. It should be noted however that the synthesis of these materials is only in its initial stages and we hope that milder intercalation conditions can be attained.

The existence of a vast range of transitions in all classes of GIC's has recently stimulated much interest in these materials. There are numerous cases in which a variety of techniques confirms the existence of certain structural or electronic changes which are not found elsewhere when studied through other experimental probes. The saturated  $\text{GaCl}_3$ -GIC's are, indeed, other such materials. The resistivity variations we have found (fig.11) as well as two others from the literature (Bach & Ubbelohde 1971a; Boissonneau & Colin 1973) show a monotonic decrease as the temperature is decreased. However, variable temperature X-ray studies clearly show a transition at about 230 K, involving both an in-plane ordering of the intercalant and a change in graphite stacking sequence from A/A/A... to A/B/A/B... as the temperature is decreased. These two transformations are probably slow, as proved by X-ray analyses carried out on thermally cycled samples. These results are indicated above (§ IV.2.3) and details furnished elsewhere (Nadi 1983; Vangelisti et al. 1983).

Similarly, as concerns the first stage  $\text{AlCl}_3$ -GIC's, a previous study of  $\rho(T)$  (Bach & Ubbelohde 1971b) has shown a gradual, nonlinear decrease as the temperature was lowered from 300 K, a rapid drop, followed by a more gradual, linear decrease below about 220 K; increasing the temperature from about 60 to 300 K resulted in an unchanged shape, but the rapid variation occurred at about 240 K and hysteresis was evident over the entire temperature range. Some years later, DTA experiments revealed an equivalent reversible phenomenon between 200 and 250 K (Baiker et al. 1981). In none of our experimental runs, including those on two first stage compounds did we find evidence for this transition. As was noted above (§IV-2-2) depending on the exact conditions of preparation, it is possible to synthesize materials in which the intercalant is either ordered or disordered, the compounds possessing different values of interplanar distance. If the above comments on  $\text{GaCl}_3$  GIC can be applied to their  $\text{AlCl}_3$  counter parts, then the results suggest that the previous studies (resistivity, DTA) were carried out on the disordered variety, which ordered as the temperature was decreased.

While the general shape of the  $\rho(n)$  variation (Fig 10a) determined for the  $\text{GaCl}_3$  family is similar to what we have indicated elsewhere for the alkali metal GIC's (McRae et al 1980b), a precise explanation is lacking, due to the numerous intervening factors.

First of all, it has been established both theoretically and experimentally that the charge distribution along the  $\vec{c}$ -axis is inhomogeneous to such an extent that neither of the two extreme, simplifying charge distribution models is correct : neither the rigid band case nor the intercalant + bounding layer sandwich model. There is a non negligible charge transfer to non-intercalant bounding layers, particularly to the second nearest neighbours. The exact transfer to this layer lies between  $\sim 2$  and  $\sim 15\%$ . It should be noted that the theoretical works point out that the exact value varies with the absolute value of  $f$ , the number of electrons transferred per intercalant entity (atom, molecule). Most experimental techniques show, indeed, that  $f$  is a stage dependent parameter. The mobility of these carriers has not been determined but even qualitatively it is evident that the total conductivity will integrate contributions from several layers, each with its own carrier density and mobility.

A second factor which is primordial to the understanding of the resistivity variations ( $\rho(n)$  and  $\rho(T)$ ) is the density and type of faults introduced through the intercalation process itself. As has been indicated above, certain intercalants provoke a significant increase in mosaic spread or even more massive destruction of the host. This is true of the  $\text{TlCl}_3$  compound, in which both the residual and room temperature resistivities are much greater than those of the other metal trichloride GIC's. Furthermore, while in first stage compounds all the interstices are completely filled, this is not so in any higher stage products. It is generally accepted that the space between any two successive carbon layers is partially filled and that each graphite plane is pleated (Daumas-Herold model). These pleats then correspond to dislocations, the density of which depends on the stage index  $m$ , the exact preparation conditions, etc. A third type of fault is stacking disorder as outlined above (& IV.2.1.). All of these faults may co-exist in a given sample and while efforts can be made to choose reaction conditions which assure as little defect formation as possible, this remains a difficult element to fully control particularly inasmuch as different graphites may react differently under identical conditions.

A third consideration is also of importance and this relates to the chemical formulation of the compounds. It was long believed that the intercalant and stage uniquely characterized a compound. More recently, it has been shown that for a given stage material, wide variations in intercalant density can exist from sample to sample. This is particularly true in the case of the higher stage materials.

(e.g.  $\text{GaCl}_3$  GIC, for  $n \geq 4$ ). On the  $\rho(n)$  curves, this constitutes a plausible explanation for the existence of similar values of  $\rho$  for several successive stage materials. It should further be noted that the metal trichloride materials are, in fact, non stoichiometric ternary compounds containing graphite, the trichloride and chlorine.

#### IV.5. Diverse

The first low temperature resistivity studies (see First Annual Report) were made on the graphite- $\text{HNO}_3$  GIC's of the  $\beta$  variety (Fuzellier et al. 1981). It was shown that the lambda transition at  $\sim 250$  K characteristic of all  $\alpha$  type compounds (for  $n \leq 10$ ) is nonexistent in the  $\beta$  GIC's. The RRR of  $\text{HNO}_3$  poor compounds ( $n = 6$ ) was shown to be  $\sim 5$ , comparable to that of the trichloride GIC's but considerably lower for stage 3 materials.

# V. REMARKS CONCERNING THE THERMAL EXPANSION OF THE G.I.C.

Table 5 regroups a certain number of the thermal expansion parameters (plus certain literature references) relative to both the donor and acceptor compounds studied up to the present. It should be noted that all values indicated are based on ZYB-HOPG. This is of importance inasmuch as the exact type of graphite can influence both the  $c^*$  axis repeat distance,  $I_c$ , and its thermal variation. The mosaic spread of ZYB HOPG is given by Union Carbide as  $0.8 \pm 0.2^\circ$ ; intercalation always increases this value, but in our studies, it always remains inferior to  $2^\circ$ .

The table indicates the values of  $I_c$  at 295 and 10 K based on high index 001 Bragg reflexions. There is a high degree of precision due to the presence of the diamond powder reference (& II.2).

As regards the coefficients of thermal expansion,  $\alpha_c$ , all values are superior to that of HOPG except those of  $CsC_8$ , the rare earth compounds  $YbC_6$  and  $EuC_6$  and the alkaline earth material,  $BaC_6$ . Taking into account the precision on  $\alpha_c$  for the heavy alkali metal compounds, our values and those of Hardcastle and Zabel are in satisfactory agreement, except in the case of  $CsC_8$  (& III). There are no comparative values in the literature for the tri- or dichloride compounds.

The thermal expansion coefficient,  $\alpha_c$ , steadily increases above 5 K and around 100 K attains a practically constant value for most of the materials studied. This variation has not yet<sup>been</sup> fully interpreted and further experimental studies are in progress. The change around the temperature  $T_L$  is undoubtedly related to a characteristic temperature such as  $\theta_D^*$ . However, even for structurally simpler materials such as the alkali halides which have similar variations of the lattice constant with temperature,  $\theta_D$  as determined by elastic constant measurements or specific heat data, is not linked in an obvious manner to the experimental  $\alpha(T)$  data (see, for example, Leibfried and Ludwig 1961). Furthermore, it should be noted that the conductivity anisotropy of the materials of Table 5 spans about four orders of magnitude (from  $\sim 20$  for  $KC_8$  to  $> 105$  for the trichloride compounds). As indicated in & IV-3, the basal plane resistivity cannot be explained by a simple Bloch-Grüneisen analysis which would have allowed determining an "in-plane Debye temperature",

\* For the GIC's, the few specific heat studies show considerable scatter in the values determined for  $\theta_D$ .

Compounds	Ic 295 K	Ic 10 K	$\alpha_c 10^{-6} \text{ K}^{-1}$ 300-200 K	T <sub>L</sub>
ZYB-HOPG	3.3505 $\pm$ 0.0010	3.3355 $\pm$ 0.0010 3.3299 (a)	26 $\pm$ 1 24 $\pm$ 4 (a) 27 (c)	112
KC <sub>8</sub>	5.347 $\pm$ 0.003	5.300 $\pm$ 0.002 5.2718 (a)	39 $\pm$ 2 45 $\pm$ 8 (a)	80
KC <sub>24</sub>	8.714 $\pm$ 0.003	8.659 $\pm$ 0.003 8.6698 (a)	31 $\pm$ 2 36 $\pm$ 4 (a)	*
KC <sub>48</sub>	15.415 $\pm$ 0.004	15.340 $\pm$ 0.004	26 $\pm$ 2	110
RbC <sub>8</sub>	5.642 $\pm$ 0.003	5.604 $\pm$ 0.004 5.6102 (a)	33 $\pm$ 2 30 $\pm$ 7 (a)	95
CsC <sub>8</sub>	5.929 $\pm$ 0.003	5.910 $\pm$ 0.003 5.9137 (a)	19 $\pm$ 2 28 $\pm$ 6 (a)	
LiC <sub>6</sub>	3.698 $\pm$ 0.003	3.674 $\pm$ 0.003	31 $\pm$ 2	90
YbC <sub>6</sub>	4.564 $\pm$ 0.003	4.543 $\pm$ 0.003	20 $\pm$ 2	120
EuC <sub>6</sub>	4.867 $\pm$ 0.003	4.857 $\pm$ 0.003	12 $\pm$ 2	120
BaC <sub>6</sub>	5.278 $\pm$ 0.003	5.265 $\pm$ 0.005	10 $\pm$ 2	120
GaCl <sub>3</sub>	9.540 $\pm$ 0.005		30 $\pm$ 2	120
AlCl <sub>3</sub>	9.59 $\pm$ 0.010	9.50 $\pm$ 0.010	45 $\pm$ 3	60
	9.53 $\pm$ 0.010	9.435 $\pm$ 0.010	40 $\pm$ 2	50
FeCl <sub>3</sub>	9.385 $\pm$ 0.005	-	- 35.5 (b)	-
CdCl <sub>2</sub>	9.560 $\pm$ 0.005	9.506 $\pm$ 0.005	27 $\pm$ 3	100
CoCl <sub>2</sub>	9.395 $\pm$ 0.005	9.343 $\pm$ 0.005	29 $\pm$ 3	*

(a) Hardcastle and Zabel (1983)

(b) Mazurek and Dresselhaus (1982)

(c) Bailey and Yates (1970)

\*T<sub>L</sub> undefined because of plateaus in experimental curves.

Table 5. Experimental thermal dilation data

T<sub>L</sub> is the approximate temperature at which the thermal variation curves change slope.



## VI. OVERALL CONCLUSIONS

Contract DAJA 37-81-C-0045 has substantially helped our laboratory in developing certain sectors of graphite intercalation compound research, notably in the fields of crystallography and electrical conductivity.

The room temperature crystallography studies have brought out the nature of different kinds of intrinsic disorder. In the second stage alkali metal GIC's, for instance, the metal atoms appear to be extremely mobile; only a fraction of them statistically occupy sites which are well defined relative to the graphite sheets. This thermally activated disorder cannot be avoided. The room temperature work has furthermore allowed a quantitative evaluation of certain types of defects. In a first stage compound such as  $\text{KC}_8$  and even more so in the metal halide compounds such as those of  $\text{FeCl}_3$ , intercalation can provoke major, quite macroscopic, defects such as increased mosaic spread and the introduction of stacking faults along the  $\vec{c}$  axis. It should be possible to reduce or at least minimize this type of defect through better or more gentle intercalation processes.

It has not yet proved possible to carry out complete structural analyses at low temperature. However, the variation of the  $\vec{c}$  axis repeat distance as a function of temperature has been evaluated with a high degree of precision. This study has provided the most complete set of thermal expansion data available on graphite intercalation compounds.

As regards the electrical measurements, the variation of resistivity with stage and temperature for the  $\text{GaCl}_3$  family is also the most extensive characterization of any family of GIC's.

Correlation between all of these studies is obviously of much interest. This has been attempted particularly as regards the various types of transitions. As indicated above, the crystallographically determined order-disorder transition of the saturated  $\text{GaCl}_3$  GIC is not found in the same compounds when studied using resistivity measurements; however, a most unexpected  $\rho(T)$  slope change was found in seventh stage products at temperatures corresponding to the first stage crystallography changes. In other cases, conductivity and crystallography studies often do allow correlating anomalous behaviour; for the second stage potassium compounds, the thermal expansion as well as the conductivity studies show anomalous behaviour in the same temperature regions. The  $I_c(T)$  data relative to the  $\text{CoCl}_2$  GIC suggest some sort of transition which has yet to be verified through other experimental probes.

Theoretical work is currently under way so as to attain better understanding of the experimental results.

In conclusion, we would like to acknowledge the E.R.O. for its financial support. Several significant results have been obtained (see list of references) and the work which was stimulated by this contract will now be expanded upon, based on the acquired knowledge and experience.

# APPENDIX

## Determination of the thermal expansion coefficient of the $M^+$ ions from that of metallic halides

The  $\frac{\Delta L}{L_{295}} = f(T)$  curves, relative to KCl and CsCl are shown on fig. 12. Their shape is similar to that of the graphitides and presents a quasi-linear portion.

We suppose that the dilatation of each  $M^+$  and  $X^-$  ion is proportional to the radius. The value of the expansion coefficient  $\alpha_{M^+}$  is given by :

$$\alpha_{M^+} = \frac{\alpha(M^+X^-)}{m + \frac{(1-m)^2}{m}}$$

where  $m$  represents the fractional contribution of the  $M^+$  to the  $M^+X^-$  distance.

The  $\alpha_{M^+}$  and  $\alpha_{X^-}$  are given in the following table :

Ion	$\bar{\alpha}_{120-300 \text{ K}}$	Ion	$\bar{\alpha}_{120-300 \text{ K}}$
$\text{Li}^+$	$(11.9 \pm 0.4) 10^{-6} \text{K}^{-1}$	$\text{F}^-$	$(27.8 \pm 1.6) 10^{-6} \text{K}^{-1}$
$\text{Na}^+$	$(21 \pm 1.2) 10^{-6} \text{K}^{-1}$	$\text{Cl}^-$	$(38.3 \pm 3) 10^{-6} \text{K}^{-1}$
$\text{K}^+$	$(27.5 \pm 1) 10^{-6} \text{K}^{-1}$	$\text{Br}^-$	$(41.8 \pm 2.4) 10^{-6} \text{K}^{-1}$
$\text{Rb}^+$	$(33 \pm 0.6) 10^{-6} \text{K}^{-1}$	$\text{I}^-$	$(46.9 \pm 1.4) 10^{-6} \text{K}^{-1}$
$\text{Cs}^+$	$(36 \pm 2) 10^{-6} \text{K}^{-1}$		

Table 6. Thermal expansion coefficients of the  $M^+$  and  $X^-$  ions in metallic halides.

The dispersion of the values is relatively large, correlated with different sizes of the associated ion.

# References

(Note : the references indicated by (x) were partially funded by this ERO contract)

- Bach B. & Ubbelohde A.R. 1971 a. "Chemical and electrical behaviour of graphite-metal halide compounds", *J. Chem. Soc. A* **23**, 3669
- Bach B. & Ubbelohde A.R. 1971 b. "Synthetic metals based on graphite-aluminium halides", *Proc. Roy. Soc. A* **325**, 437.
- Baiker A., Habegger E., Sharma V.K. & Richarz 1981 "Order-disorder transformation of graphite-aluminium chloride intercalation compounds" *Carbon* **19**, 327
- Bailey A.C. & Yates B. 1970 "Anisotropic thermal expansion of pyrolytic graphite at low temperature" *J. Appl. Phys.* **41**, 5088
- Boissonneau J.F. & Colin G. 1973 "Conductibilité des composés d'insertion d'un pyrocarbone avec le brome, le chlorure de Fe<sup>III</sup> et le chlorure de Ga<sup>III</sup>" *Carbon* **11**, 567
- Fuzellier H., Rousseaux F., Maréché J.F., Mc Rae E. & Hérold A. "Chemical and Physical properties of new graphite-HNO<sub>3</sub> compounds" *Proc. 15th Bien. Conf. Carbon (Philadelphia)* p. 393
- (x) Guérard D., Takoudjou C. & Rousseaux F. 1983 "Insertion d'hydruure de potassium dans le graphite" *Synth. Met.* **7**, 43.
- Hardcastle S.E. & Zabel H. 1983 "Thermal expansion and lattice anharmonicity of alkali-graphite intercalation compounds" *Phys. Rev. B* **27**, 6363
- Lagrange P., Guérard D. & Hérold A. 1978 "Sur la structure du composé KC<sub>8</sub>" *Ann. Chim. Fr.* **3**, 143.
- Laplume J. 1955 "bases théoriques de la mesure de la résistivité et de la constante de Hall par la méthode des pointes" *Onde Elect.* **35**, 113.
- Leibfried G. and Ludwig W. in "Solid State Physics", edited by F. Seitz and D. Turnbull (Academic, New York, 1961), Vol. 12.
- (x) Maréché J.F., Mc Rae E., Nadi N. & Vangélisti R., 1983 "Comparative study of electrical resistivity of metal trichloride intercalated graphite" *Synth. Met.* **8**, 163.
- Mazurek H., Ghavamishahidi G., Dresselhaus G. & Dresselhaus M.S., 1982 "Low temperature X-ray diffraction study of stage 1 graphite-FeCl<sub>3</sub>" *Carbon* **20**, 1982.
- Mc Rae E., Maréché J.F. & Hérold A., 1980 a. "Contactless resistivity measurements : a technique adapted to graphite intercalation compounds" *J-Phys. E: Sci. Instrum.* **13**, 241.
- Mc Rae E., Billaud D., Maréché J.F. & Hérold A. 1980 b. "Basal plane resistivity of alkali metal-graphite compounds" *Physica* **99 B**, 489.

- (x) Mc Rae E., 1982 "Contribution à l'étude de la résistivité électrique des composés lamellaires du graphite" Thèse d'état, Université de NANCY I.
- (x) Nadi N. 1983 "Contribution à l'étude des composés du graphite avec les trichlorures des éléments III B" Thèse de 3ème cycle, Université de NANCY I
- (x) Nadi N., Vangélisti R. & Hérold A., 1983 "Caractérisation chimique et structurale des composés graphite-trichlorure de gallium Synth. Met. 7, 125.
- Onn D.G., Foley G.M.T. & Fischer J.E., 1977 "Resistivity anomalies and phase transitions in alkali metal graphite intercalation compounds" Mat. Sci. Eng. 31, 271.
- Plançon A., Rousseaux F., Tchoubar D., Tchoubar C., Krinari G. & Drits V.A., 1982, "Recording and calculation of hk rod intensities in case of diffraction by highly oriented powders of lamellar samples" J. Appl. Cryst. 15, 509
- Rossat-Mignod J., Wiedenmann A., Woo K.C., Milliken J.W. & Fischer J.E., 1982 "First order phase transition in the graphite compound  $\text{LiC}_6$ " Solid State Comm. 44, 1339.
- (x) Rousseaux F., Plançon A., Tchoubar D., Guérard D. & Lagrange P., 1981  
a. "Ordering in graphite intercalation compounds by means of X-ray diffraction" Solid State Sci. 38, 228.
- (x) Rousseaux F., Vangélisti R., Lelaurain M., Hérold A., Plançon A. & Tchoubar D., 1981 b. "X-ray structural study of graphite- $\text{FeCl}_3$  compounds" Proc. 15th Bien. Conf. Carbon (Philadelphia) p. 377.
- (x) Rousseaux F., Vangélisti R., Plançon A. & Tchoubar D. 1982 "Etude quantitative par diffraction des rayons X des corrélations entre couches dans les composés graphite-chlorure ferrique de 1er et 2ème stades" Rev. Chim. Min. 19, 572.
- (x) Rousseaux F., Tchoubar D., Tchoubar C., Guérard D., Lagrange P., Hérold A. & Moret R., 1983, "Relations entre corrélations d'orientation inséré-substrat et probabilité d'occupation d'un site hexagonal du substrat, pour les composés d'insertion graphite - métaux alcalins du 2ème stade" Synth. Met. 7, 221.
- (x) Takoudjou C. 1983 "Insertion dans le graphite d'hydrures de potassium et de sodium" Thèse de 3ème cycle, Université de Nancy I
- (x) Vangélisti R., Nadi N. & Lelaurain M., 1983 "Structures bidimensionnelles des composés du graphite avec les trichlorures des éléments III<sub>B</sub> (Al, Ga, In, Tl): analyse à basse température" Synth. Met. 7, 297
- Wu T.C., Vogel F.L., Pendrys L.A. & Zeller C. 1981 "Electrical resistivity of graphite- $\text{SbF}_5$ " Mater. Sci. Eng. 47, 161
- Zeller C., Pendrys L.A. & Vogel F.L. 1979 "Electrical transport properties of low stage  $\text{AsF}_5$  graphite intercalation compounds" J. Mater. Sci. 14, 2241.

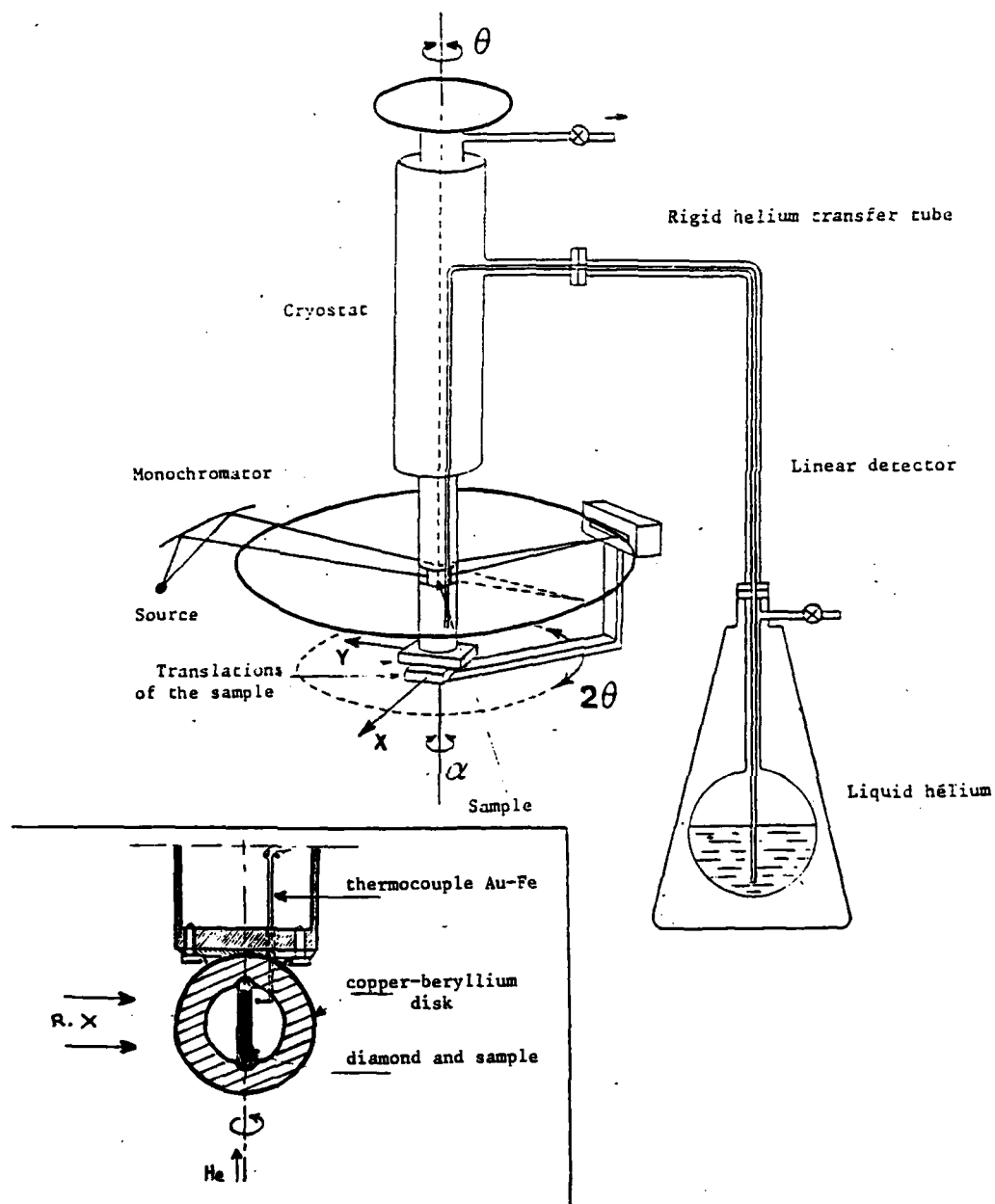


Fig. 1. Low temperature X-ray apparatus. Inset shows sample positioning.

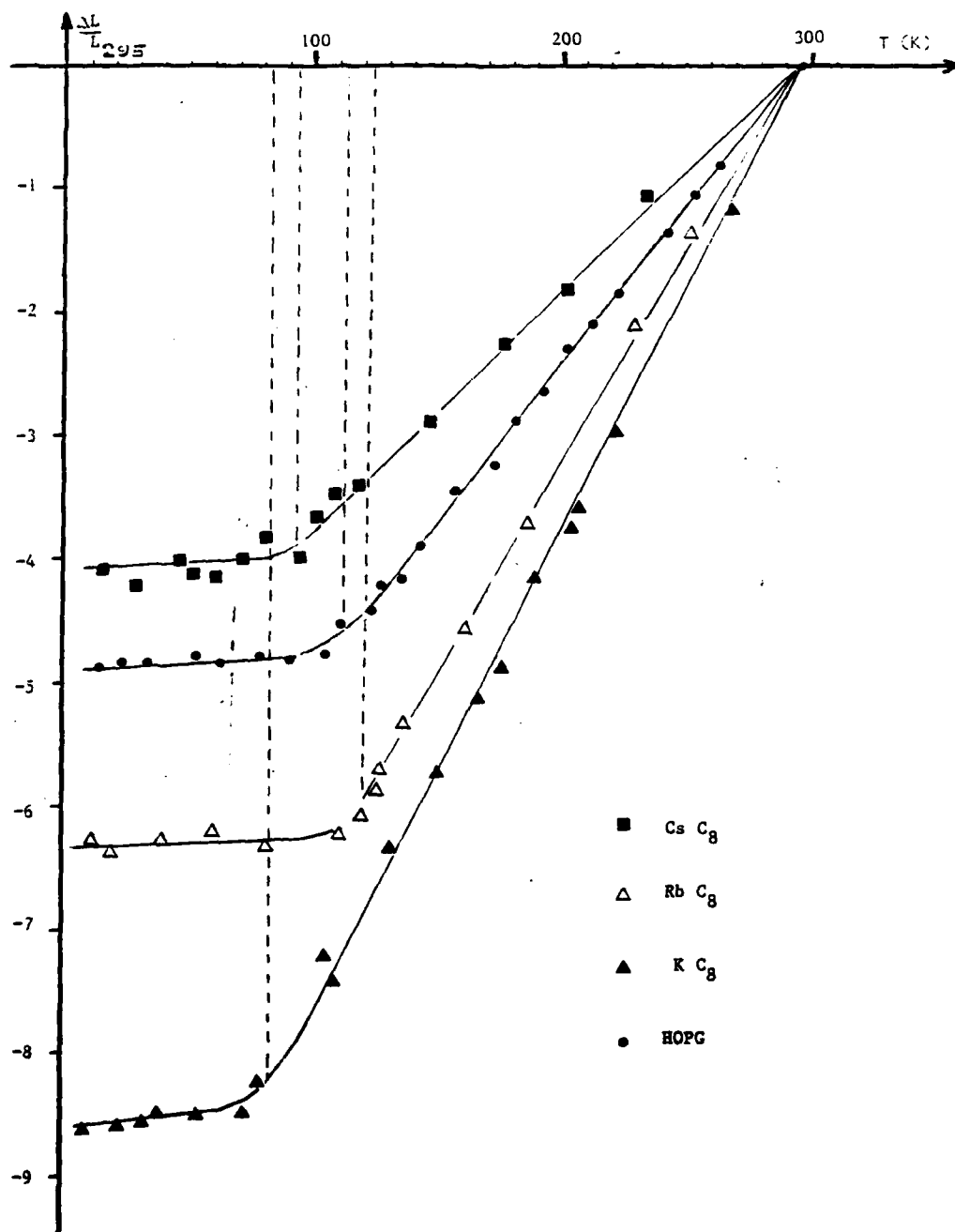


Fig. 2. Thermal expansion of first stage heavy alkali metal compounds,  $\text{MC}_8$ .  $L_{295}$  is the C axis parameter at 295 K.

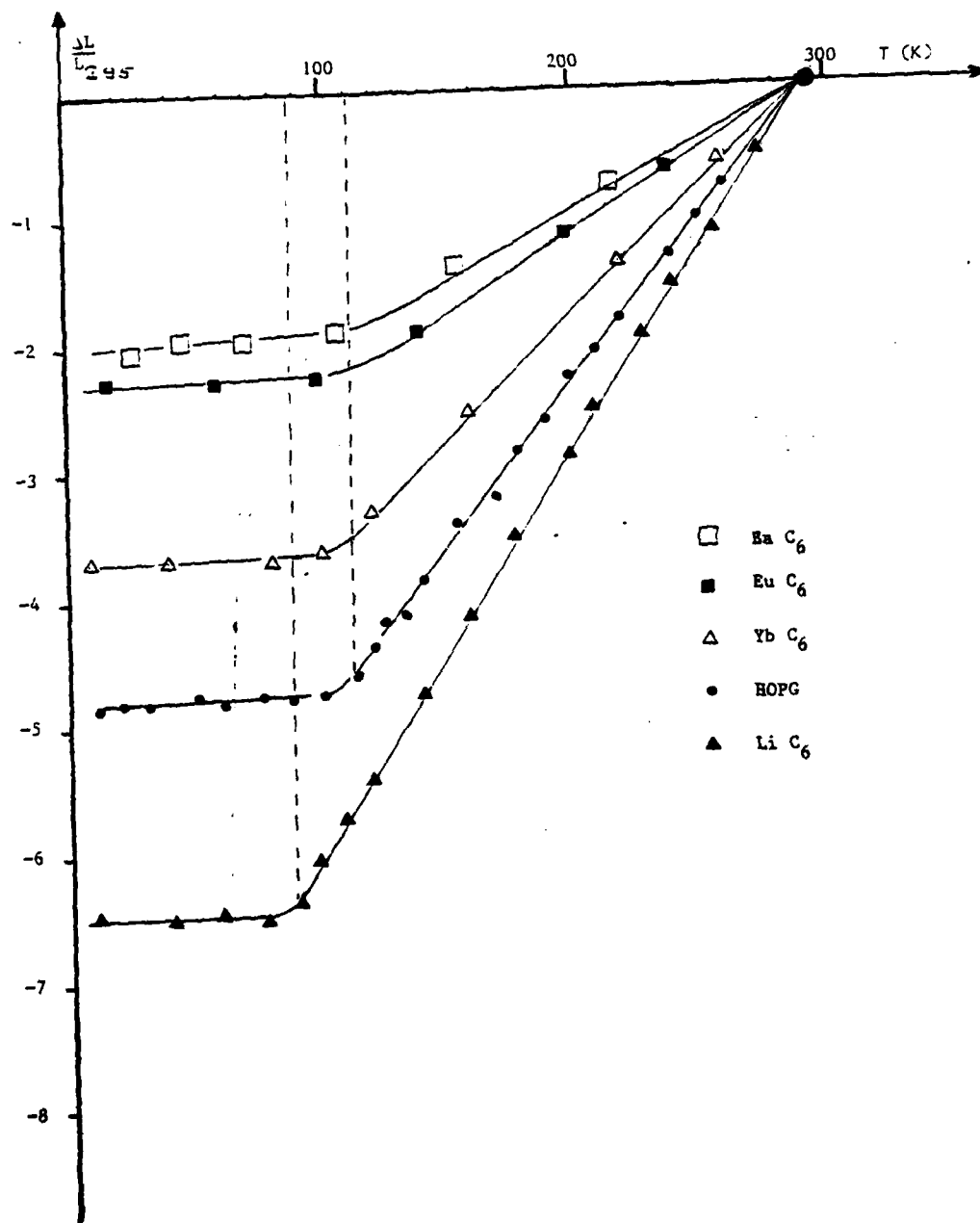


Fig. 3. Thermal expansion of first stage  $\text{MC}_6$  compounds.



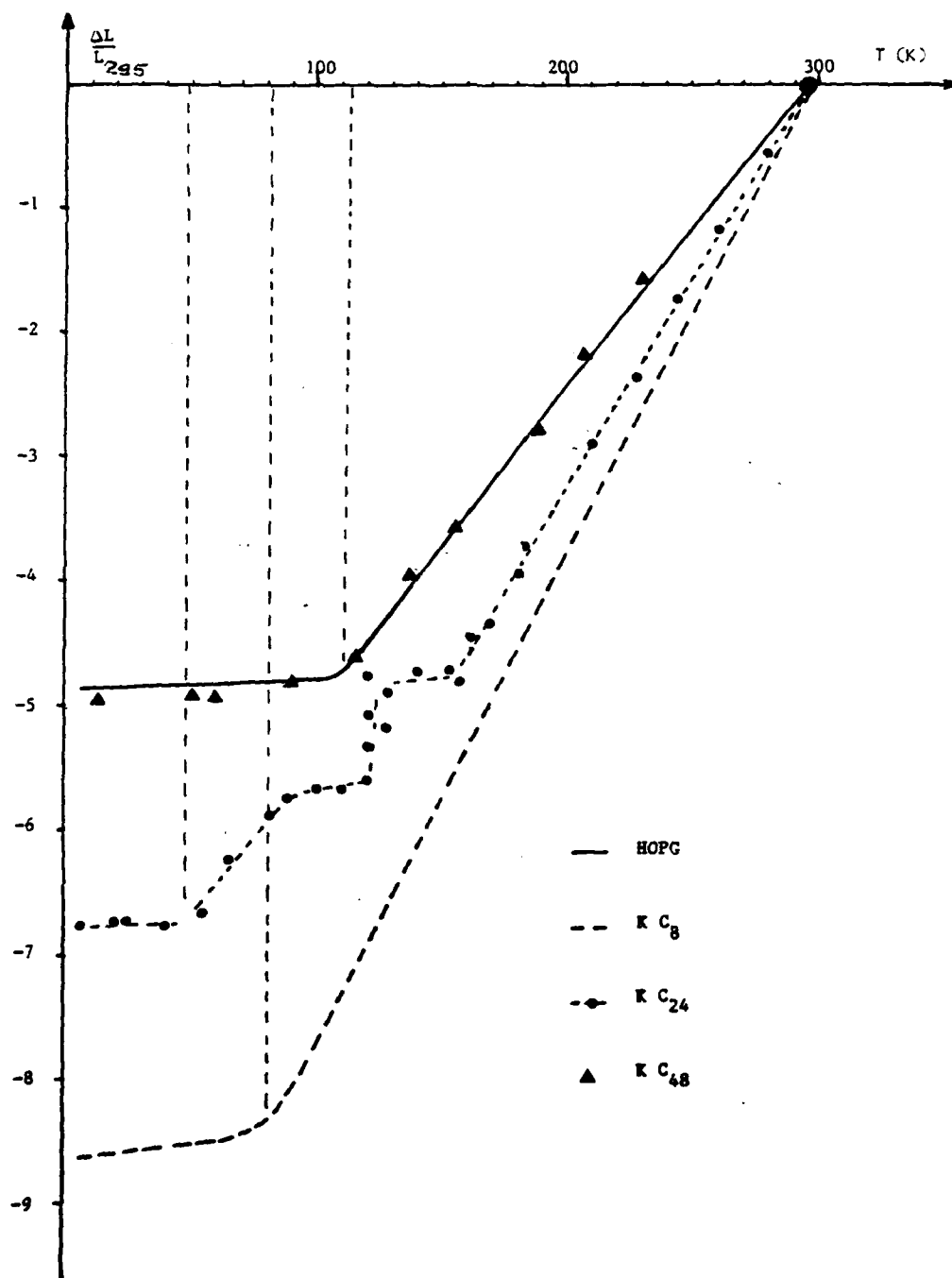


Fig. 4. Thermal expansion for 1st, 2nd and 4th stage potassium compounds.

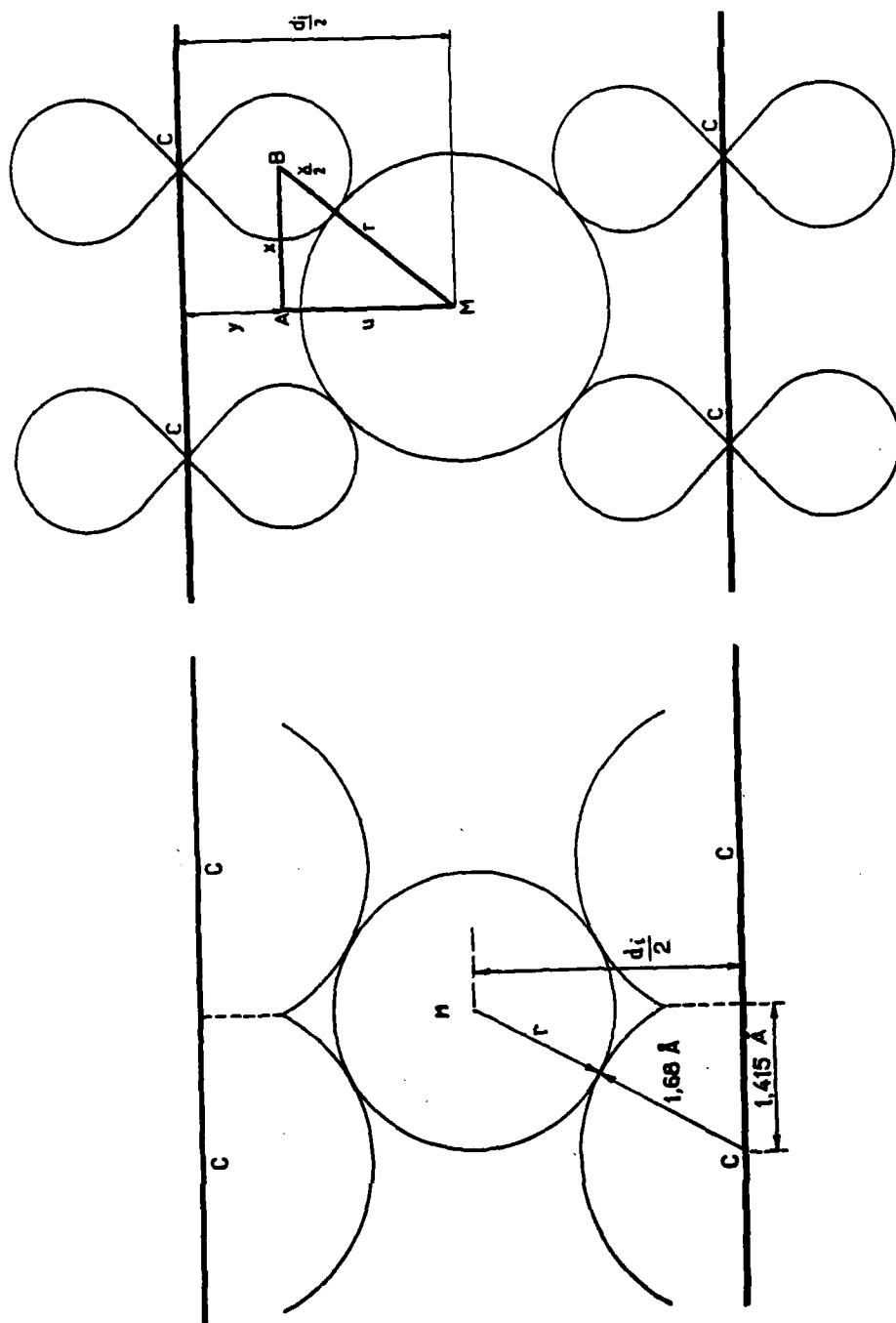


Fig. 5. Models used for calculating the expansion of the intercalant sandwich.

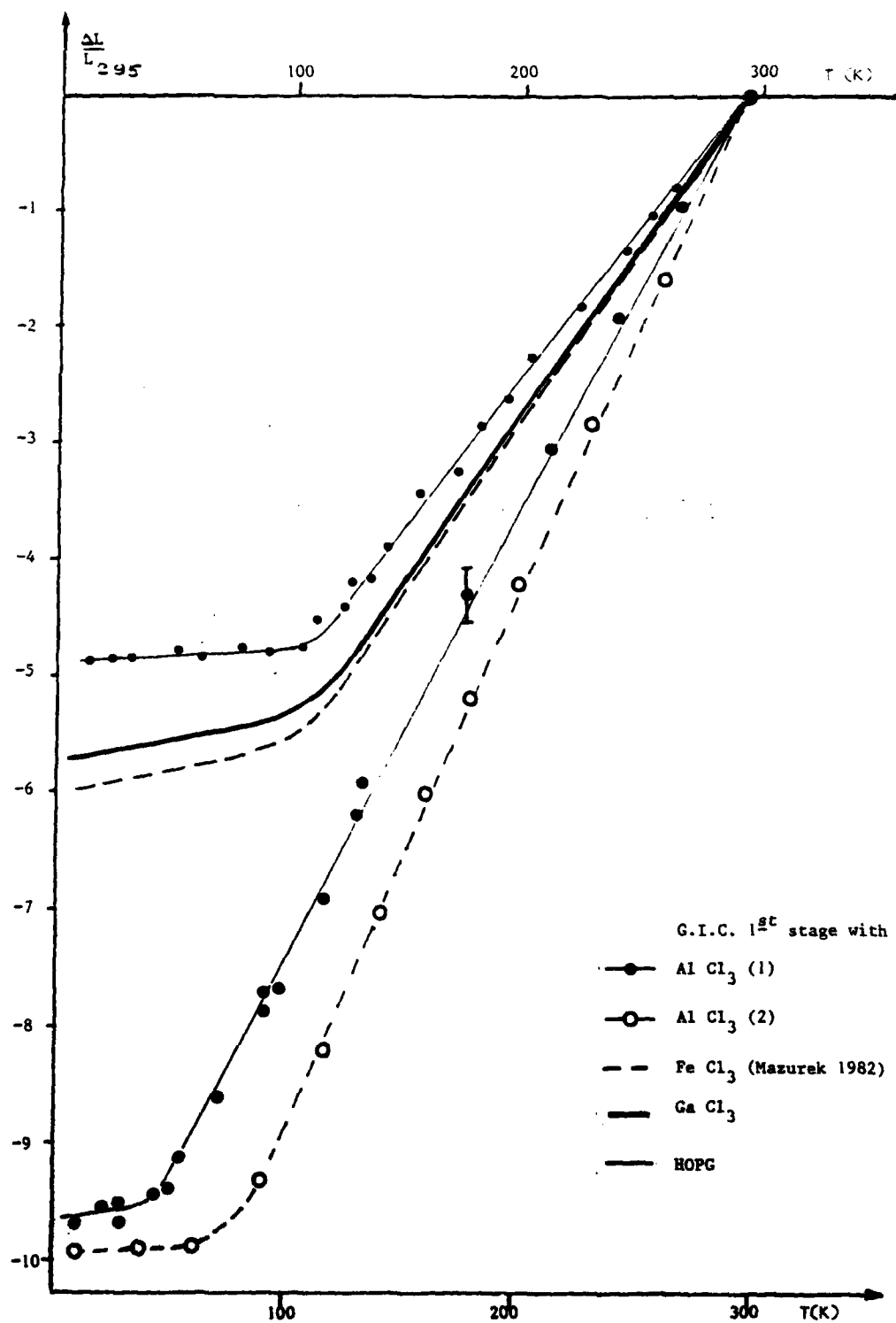


Fig. 6. Thermal expansion for first stage metal trichloride compounds.

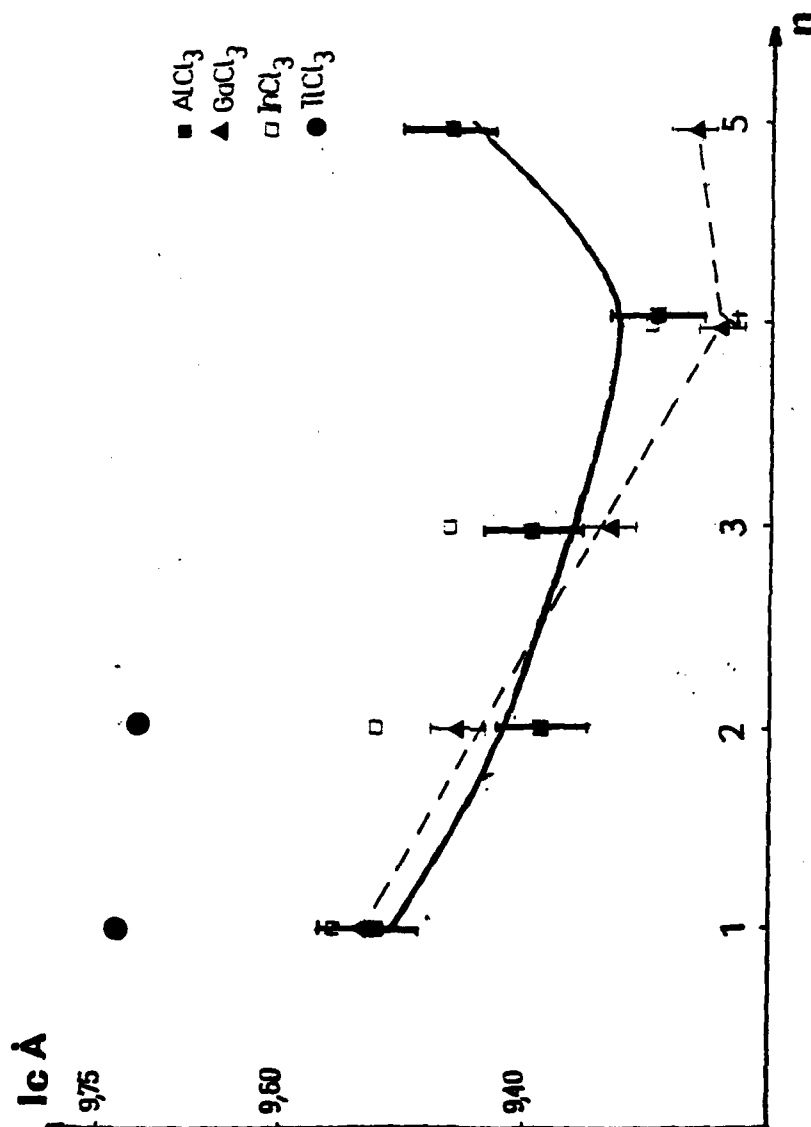


Fig. 7. Variation of interplanar distance with stage at 295 K for metal trichloride GIC's.

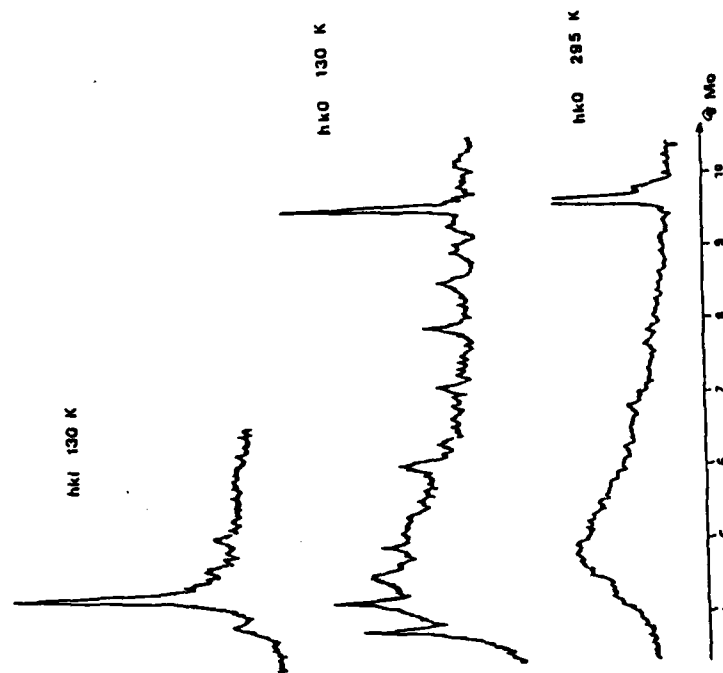
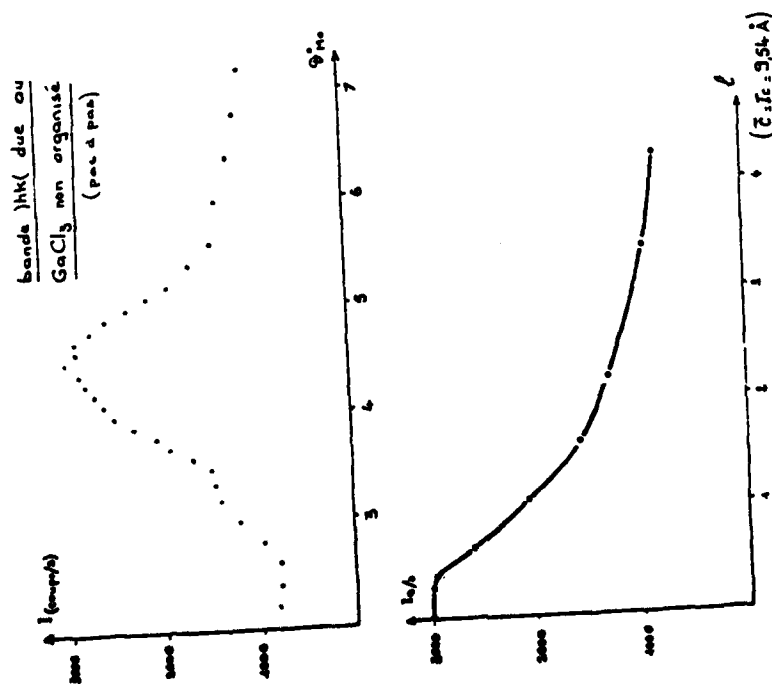


Fig. 8. (a)  $\theta$ - $2\theta$  scanning of an  $hk0$  band in unorganized  $\text{GaCl}_3$  GIC ( $n=1$ ) at 295 K (upper) and corresponding scan along  $\hat{Z}$  (lower).  
(b)  $hkl$  scans at different temperatures

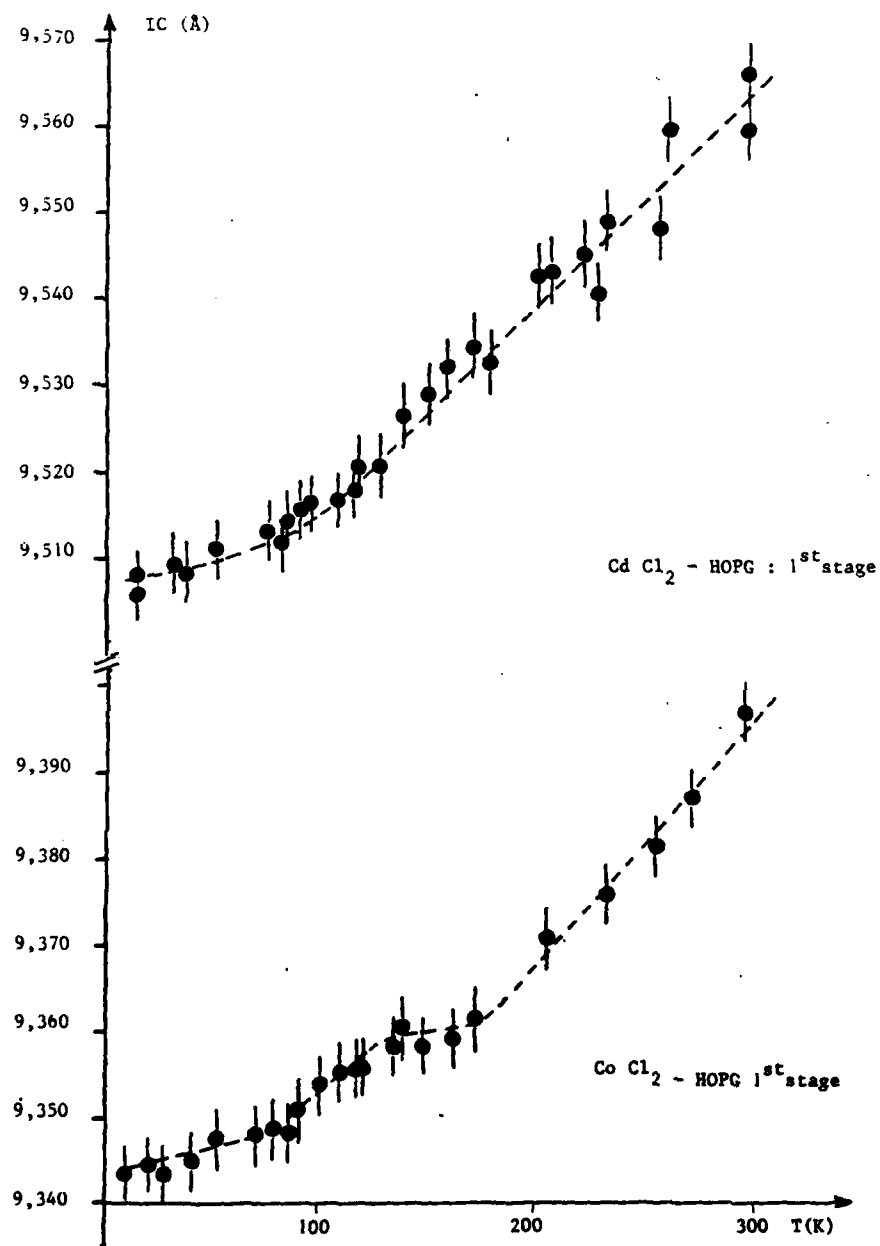


Fig. 9. Interplanar repeat distance versus temperature for dichloride GIC's.

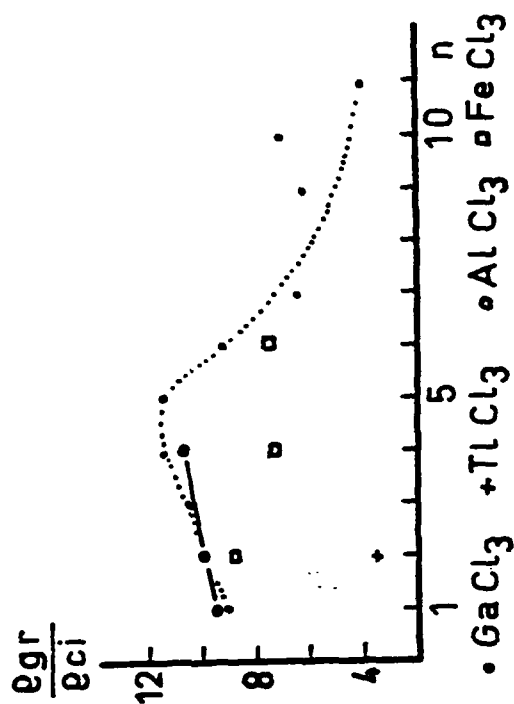
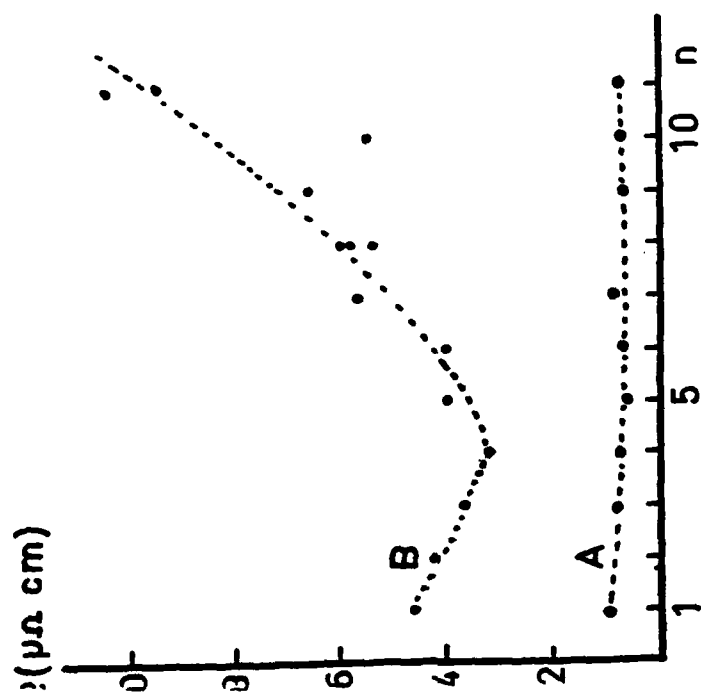


Fig. 10. (a) Residual (A) and 300 K (B) resistivity versus stage for  $\text{GaCl}_3$  GIC's.  
(b) Conductivity gain (300 K) versus stage.

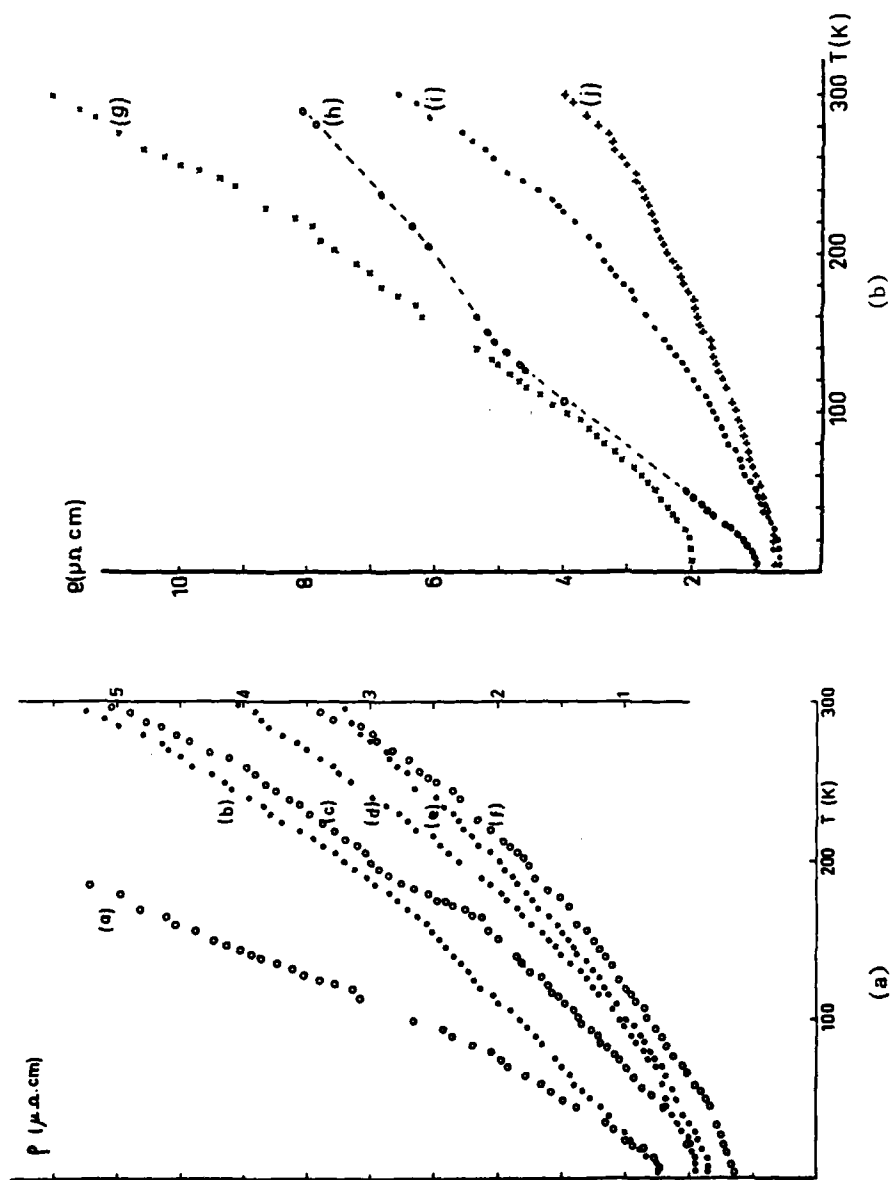


Fig. 11. Resistivity versus temperature :

(a) GaCl<sub>3</sub>-GIC's; stages as follows : (a) 11 (b) 10, (c) 7, (d) 1, (e) 3, (f) 5. Right hand coordinate axis for (a) and (b).

(b) GaCl<sub>3</sub> (h) 13 + graphite (i) 9 (j) 6

(c) top to bottom = FeCl<sub>3</sub>  $n = 6.4$ ; AlCl<sub>3</sub>  $n = 1, 2, 4$ . (page 38).

TlCl<sub>3</sub> (g) 2



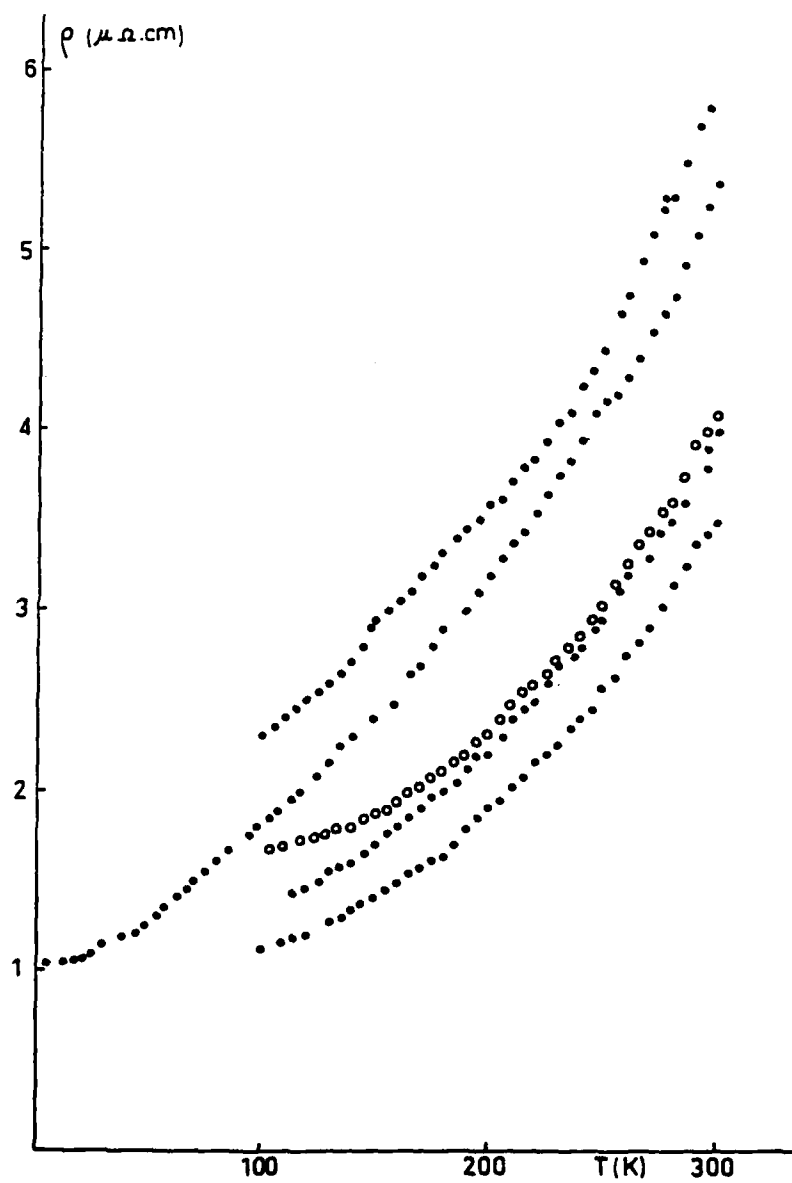


Fig. 11. (c)

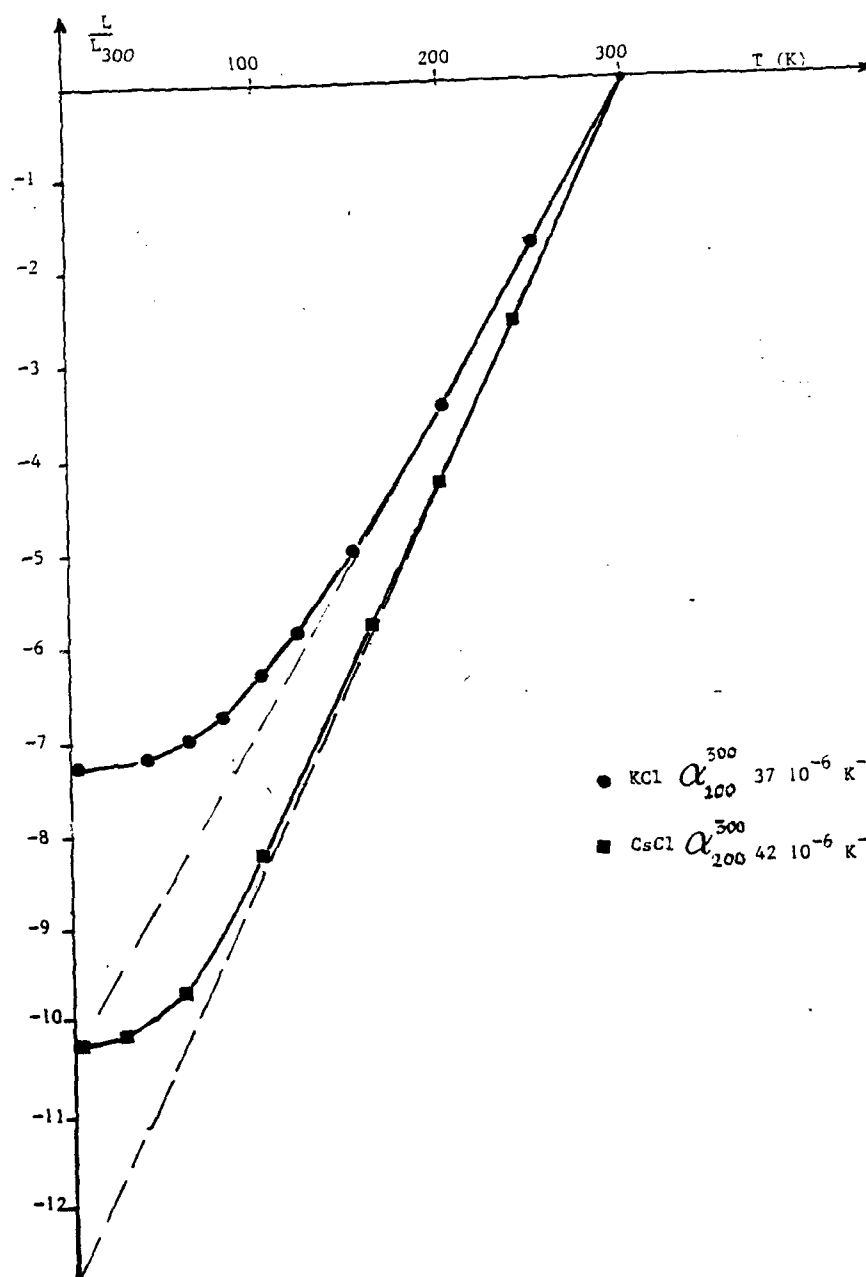


Fig. 12.  $\Delta L/L_{295}$  as a function of temperature KCl, CsCl (experimental results of this study).

END

DATE  
FILMED

6 84

DTA